STUDIES ON STRUCTURAL, OPTICAL AND ELECTRICAL PROPERTIES OF Zn-DOPED PbS NANOCRYSTALLINE THIN FILM

M. AMIR HUSSAIN[a,*], L. RAJEN SINGH[b], S. RANIBALA DEVI[c]
[a]Department of Physics, Imphal College, Imphal-795001, India
[b]Department of Physics, D.M. College of Science, Imphal-795001, India
[c]Department of Physics, Presidency College, Motbung-795107, India

The Zn-doped nanocrystalline lead Sulphide (PbS) thin films of different doping concentration are prepared by chemical bath deposition (CBD) technique. The thin films are deposited onto the glass substrates at pH value 10 and bath deposition temperature 318K. The X-ray diffraction revealed that the prepared films are polycrystalline in nature and calculated crystallites sizes decrease from 24nm to 15nm with increasing Zn- doping concentration. The scanning electron microscopy (SEM) images showed that the films comprise of grains of spherical shape of unequal size and also observed that the small particles aggregate together to form a larger cluster. The optical properties are determined from UV- visible spectroscopy measurement in the range of 320nm to 900nm and calculated optical band gap is found in between 2.15eV to 2.21eV. The electrical conductivity of the prepared thin films is found to be in the order of $10^{-4}\Omega^{-1}cm^{-1}$.

1. Introduction

In the last decades, the members of group IV-VI nanocrystalline semiconductor thin films have been focus of scientific research due to their future applications in the diverse fields of science and technology [1-5]. These materials have unique optical, electrical, magnetic and chemical properties and also change their properties significantly by changing the grain size and thickness of the film [6, 7]. The unusual properties of the nanocrystalline semiconductor thin films are due to quantum confinement effect and surface effect [8]. One of the main factors driving the current interest for semiconducting nanocrystalline thin film is due to the fact that optimization of devices such as solar cells, supercapacitors, photocatalytic coatings and electrochromic windows requires control of the physical and chemical properties of the employed materials [9-11]. Among the semiconductor compounds, PbS is a group IV-VI semiconductor compound with a narrow band gap of 0.41eV at 300K and having large exciton bohr radius (18nm) and consider an ideal semiconductor compound for future applications like solar cells, photochemical cells, optoelectronics devices etc. [12]. Zn-doped nanocrystalline PbS thin films have been synthesized by different techniques such as chemical bath deposition [13, 14], electro-deposition, spray pyrolysis, SILAR, physical vapour deposition, inert gas condensation, laser ablation, chemical vapour deposition, etc. [15-18]. Mengting Liu et al. [19] reported that the band structure of Zn-doped PbS nanopowder changes due to the incorporation of Zn on the PbS thin films. Faraj et al. [20] prepared the Zn-doped PbS thin films by chemical spray pyrolysis and the structural, morphological and electrical properties of the prepared films. The crystallites size of the films decreases from 30.87nm to 14.73nm and surface roughness of the film also decrease with increase in Zn doping concentration. Mengting Liu et al. [21] reported the effect of Zn-doping concentration on optical band gap of PbS thin films. The optical band gap of the prepared films increases with increase in Zn doping concentration.

In the present work, the Zn doped nanocrystalline PbS thin films are prepare by chemical bath deposition method which is suitable and most economic for the deposition of thin film and

---

also to investigate the effect on the structural, optical and electrical properties of the prepared films.

2. Experimental procedures

2.1. Substrates cleaning

The cleaning of glass substrates is very important in the deposition of thin film. The substrates of appropriate sizes 2 x 2 cm^2 are cut from the glass slide and washed with detergent solution, then treated in a mixture of nitric acid and isopropyl alcohol. The substrates are taken out from the solution and ultrasonically cleaned with deionized water for 30 min and wiped with acetone and heated in an oven at 150°C about 30 min for drying.

2.2. Preparation of Zn-doped PbS thin film

For the preparation of Zn-doped nanocrystalline PbS thin films, Lead Acetate $(CH_3COO)_2Pb.3H_2O$, Thiourea (CH_4N_2S) and Zinc Acetate $(Zn(CH_3COO)_2)$ purchased from Merck chemical are used as Pb^{+2}, S^{-2} and Zn^{+2} ions sources respectively. For this, 20ml of each 0.05 M lead acetate and 0.05M of thiourea are mixed together in a 100ml beaker and subsequently 1.5wt% of $Zn(CH_3COO)_2$ are added in the resultant solution and stirred for about 10min to get uniform mixture. The pH value 10 of the solution is adjusted by drop wise addition of aqueous ammonia (NH_3). The cleaned glass substrates are vertically immersed into the solution, supported by the wall of the beaker. The mixture solution is heated at 318K for 10 minutes. The colour of the solution slowly changes from brownish to dark brown after heating. The resultant solution is kept at room temperature for 3 hr for further deposition on the glass substrates. The glass substrates coated with Zn-doped PbS thin film on both sides are taken out and thoroughly washed with distilled water and dried in open atmosphere. The glass substrate surface facing the wall of the beaker during deposition is uniform and retained for further studies and the other substrate surface facing the interior of the bath is removed with a cotton swap using nitric acid solution. In the same procedure, three sets of films of different concentrations of Zn-doped nanocrystalline PbS films are prepared.
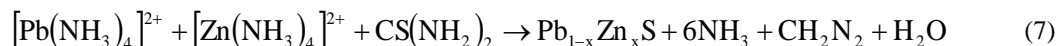
2.3. Reaction mechanism

Zn doped PbS films are prepared by adding different concentrations of zinc acetate (Zn ions source) and the reaction for the formation of $Pb_{1-x}Zn_xS$ are given as follow

$$Pb(CH_3COO)_2.3H_2O \rightarrow Pb^{2+} + 2CH_3COO^{-1} + 3H_2O \quad (1)$$

$$Pb^{2+} + 4NH_3 \rightarrow Pb(NH_3)_4^{2+} \quad (2)$$

$$Zn(CH_3COO)_2 \rightarrow Zn^{2+} + 2CH_3COO^- \quad (3)$$

$$Zn^{2+} + 4NH_3 \rightarrow Zn(NH_3)_4^{2+} \quad (4)$$

In alkaline medium dissociation of $CS(NH_3)_2$ take place

$$CS(NH_2)_2 + OH^- \rightarrow CH_2N_2 + H_2O + SH^- \quad (5)$$

$$SH^- + OH^- \rightarrow S^{-2} + H_2O \quad (6)$$

Then the overall chemical reaction is as follow

$$\left[Pb(NH_3)_4\right]^{2+} + \left[Zn(NH_3)_4\right]^{2+} + CS(NH_2)_2 \rightarrow Pb_{1-x}Zn_xS + 6NH_3 + CH_2N_2 + H_2O \qquad (7)$$

2.4. Characterization of the prepared film

The structural characterization of the prepared films are carried out by analysing the X-ray diffraction (XRD) patterns obtained using a X-PERT PRO Philips (λ= 1.5405 A^o) within the 2θ range 15-60° which is operated at 40kV and 20mA. The surface morphology and compositional analysis of the films are studied using scanning electron microscopy (SEM) JEOL-6360 operating with an accelerating voltage 20kV. The thickness of the prepared film is measured by the Tolansky method as discussed in our earlier published paper [15]. The optical properties are studied by using Carry-300 scan UV-Visible spectrophotometer and to determine the optical band gap energy. For electrical conductivity measurement 'Al' electrodes in a co-planar configuration separated by a small gap are evaporated in vacuum on the surface of the prepared film. A constant voltage is applied across the sample and the current is noted using a Keithley electrometer. The temperature on the sample surface is measured by Instron (IN 303) electronic temperature controller. The type of electrical conductivity of the films is determined by simple hot probe method [15]. For the studies of photoconductive rise and decay characteristics of the Zn-doped nanocrystalline PbS thin film, Al electrodes are vacuum deposited on the two ends of rectangular Zn-doped PbS films separated by a small gap. A constant voltage is applied to the sample through a standard resistance and is connected to the X-Y/t recorder (M/S Digital Electronics Ltd., Mumbai, India model: Omnigraphic (2000).

3. Results and discussion

3.1. Structural characterization

The XRD patterns of Zn-doped nanocrystalline PbS thin films at different doping concentrations are shown in Fig. 1. The main feature of the diffraction patterns of the prepared films are the same but only the peak intensity varies. The observed 'd' spacing and the respective prominent peaks correspond to reflection (111), (200), (220) , (311) and (222) planes which are in good agreement with the JCPDS data card (ASTM data file No. 5-5921). Therefore, it has been concluded that Zn-doped nanocrystalline PbS thin films are polycrystalline in nature with cubic structure. As we see from Fig.1, the intensity of the peaks in the diffraction pattern is found to increase with increase in doping concentration. The intensities of (111), (220) (311) and (222) peaks are low in comparison with the (200). This indicates that the orientation of the grain growth is preferably along (200) direction. The preferential orientation in the (200) direction has also earlier reported [22, 23]. The average crystallite sizes of the Zn-doped nanocrystallite PbS thin films are calculated from the full width at half maximum (FWHM) of X-ray diffraction peaks using Scherrer's formula [15]

$$D = \frac{0.94\lambda}{\beta \cos\theta} \qquad (8)$$

where λ is the X-ray wavelength, β is the full width at half maxima in radian and θ is the Bragg's diffraction angle. As a doping concentration is increased, the diffraction peaks become broader and less intense due to decrease in the crystallite size. The average crystallite size is found to decrease from 25nm to 15nm as the doping concentration increased from 1.5wt% to 2.5wt%. Since the ionic radius of Zn^{+2} (0.74Å) is less than that of Pb^{+2}(1.19 Å) [24, 25]. The lattice parameter 'a' for cubic structure is calculated using the given formula

$$d = \frac{a}{\sqrt{h^2 + k^2 + l^2}} \qquad (9)$$

and the corrected values from the Nelson –Riley plots (Fig. not shown here) are given in Table 1. The calculated lattice parameter of the PbS thin films are slightly different from the bulk value 5.936 Å. The deviation in the values of the lattice constant of the PbS films from the bulk value indicates the presence of strain in the films [26]. The misfit stress is one of the most important factor adversely affecting the structural properties which is resulted from geometric mismatch at inter phase boundaries between crystalline lattices of films and substrates [27]. These stresses can cause microstrain in the films. The microstrain and dislocation density of the Zn-doped nanocrystalline PbS films deposited at different doping concentration are calculated using the relation (10) and (11) respectively.

$$\varepsilon = \frac{\beta \cot \theta}{4} \qquad (10)$$

$$\delta = \frac{n}{D^2} \qquad (11)$$

where 'β' is the full width at the half of the maximum peak intensity (FWHM) and 'θ' is the Bragg's angle and 'n' is a factor which is equals to unity giving minimum dislocation density and 'D' is the crystallite size. The calculated values of microstrain and dislocation density are represented in the Table1. From Table 1, we see crystallite size decreases with increase in doping concentration whereas microstrain and dislocation density increase with increase in doping concentration.
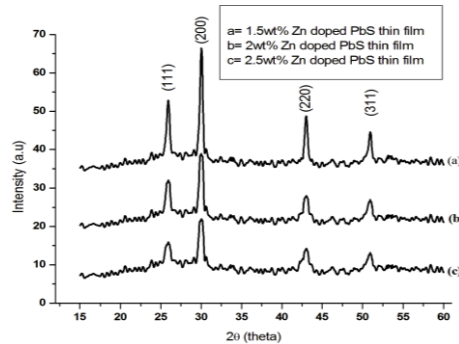

Fig. 1. XRD spectra of Zn doped nanocrystallne PbS thin film at different doping concentration.

Table 1. Structural parameters calculated from the XRD spectra of Zn-doped PbS thin film.

Zn-Doping concentration	Average crystallite sizes (nm)	Standard 'd' values (Å)	Plane	Calculated 'd' values (Å)	Calculated lattice constant 'a' ((Å)	Corrected lattice constant 'a' (Å)	Average microstrain (ε)	Dislocation density (δ) (lines/m²)
1.5wt%	24	3.429 2.969 2.099 1.790	(111) (200) (220) (311)	3.436 2.984 2.104 1.795	5.951 5.968 5.951 5.953	5.938	5.006×10^{-3}	1.736×10^{15}
2.0wt%	18	3.429 2.969 2.099 1.790	(111) (200) (220) (311)	3.438 2.984 2.104 1.795	5.955 5.968 5.951 5.953	5.941	6.912×10^{-3}	3.086×10^{15}
2.5wt%	15	3.429 2.969 2.099 1.790	(111) (200) (220) (311)	3.453 2.984 2.103 1.794	5.981 5.968 5.948 5.950	5.946	8.638×10^{-3}	4.444×10^{15}

3.2 Scanning Electron microscopy

Fig. 2(a-c) shows SEM images of Zn-doped nanocrystalline PbS thin films at 10,000x magnifications. It is seen that the surface morphologies of PbS films are almost homogeneous and well covered over the entire glass substrate without any voids. It is also observed that the films consist of irregular shaped grains of ramdom sizes and these irregular shaped nanograins are interconnected with each other to form clusters. It can be noticed that the microstructure of the films is influenced by the introduction of Zinc atoms as dopant. Depending on the increasing of Zinc concentration, the surface morphologies of the films are observed to be changed.
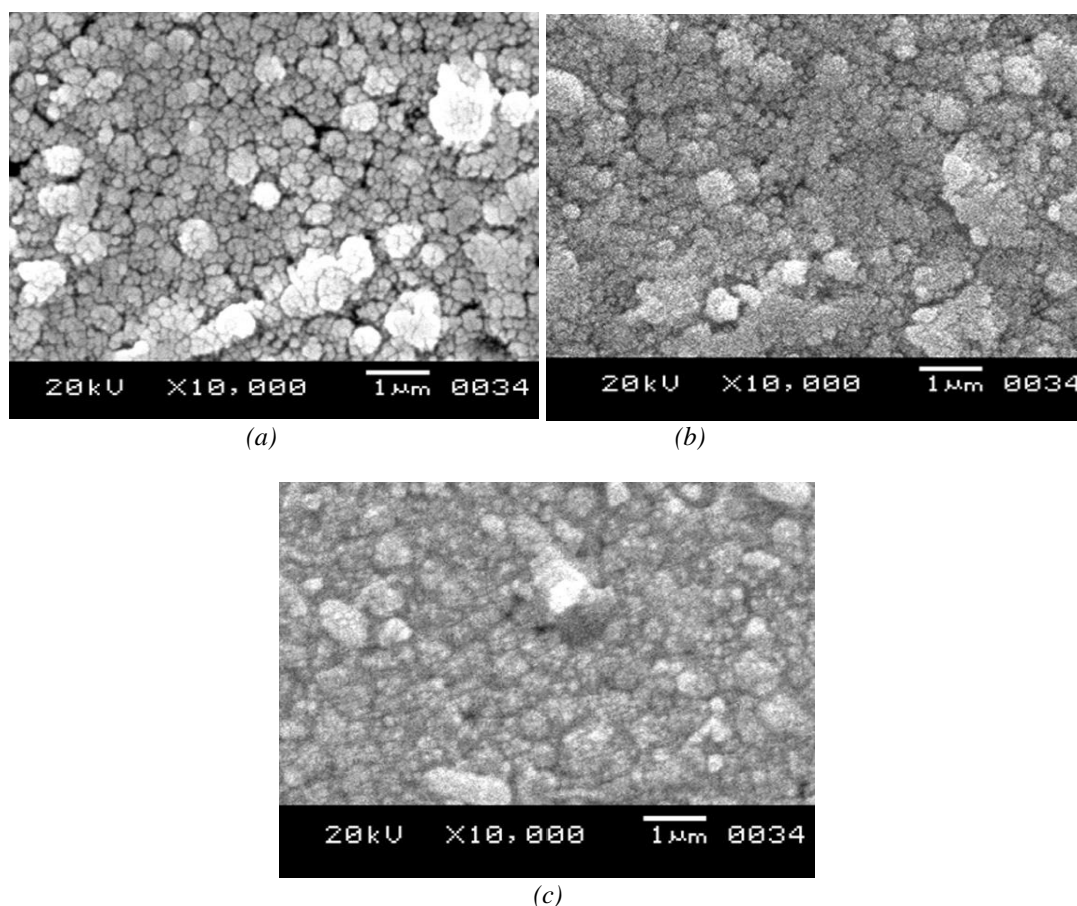
(a) *(b)*

(c)

Fig. 2. SEM photographs of the Zn doped nanocrystallne PbS thin films deposited different doping concentration (a) 1.5wt% (b) 2wt% (c) 2.5wt%.

3.3. Energy dispersive X-ray analysis (EDAX) of Zn-doped PbS films

Fig. 3(a-c) represents the EDAX spectra of the Zn-doped nanocrystalline PbS thin films at three different doping concentrations. The presence of Zn atoms in the spectra indicates that Zn atoms are incorporated with the PbS film. It is also observed that atomic percentage of Zn atoms increase with increase in Zn-doping concentration. The extra peaks observed in all the EDAX spectra correspond to Mg, Si, Na, Ca,C, O etc. which are due to glass substrate or the substrate holder used in the EDAX instrument or exposure of the film to the atmosphere. There is no source of these elements in the chemicals used for the synthesis of Zn-doped PbS film. The prominent peak observed at around 1.9 eV in the EDAX spectra belong to Si which is due to glass substrate. We consider only the atomic% of Pb and S present in the spectra and neglecting the percentage of the other elements present in the spectra.
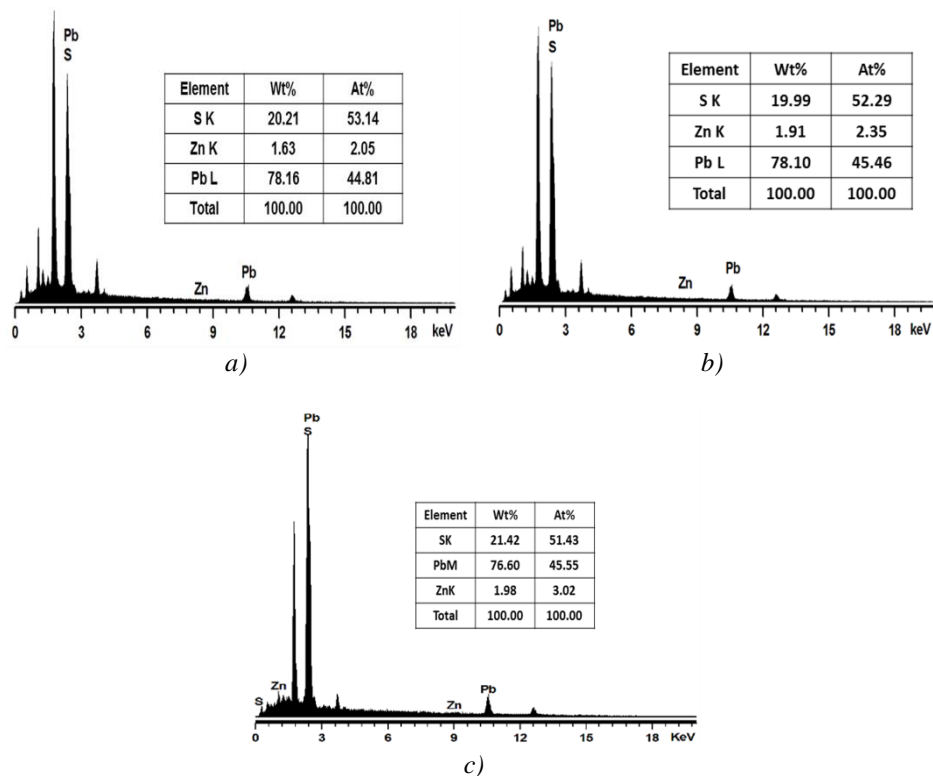
Fig. 3. EDAX spectra of Zn doped nanocrystallne PbS thin film.
a)1.5wt% Zn doped; b) 2.0wt% Zn doped; c) 2.5wt% Zn doped

3.4. Optical properties of the Zn doped nanocrystalline PbS thin films

Absorption spectra of Zn-doped nanocrystalline PbS thin films has been shown in Fig. 4 (a). From the absorbance spectra, it is seen that the absorbance of all samples have high absorption in the shorter wavelength and shifting of absorption edge towards lower wavelength with increasing in Zn doping concentration. This blue shift is indicative of the decrease of crystallite size and increase in band gap. Fig. 4 (b) represents the plot of $(\alpha h\nu)^2$ vs $(h\nu)$ of Zn doped nanocrystalline PbS thin films prepared at three different doping concentrations. The calculated optical band gap of Zn doped PbS thin films is 2.15 eV to 2.21 eV. It is observed that the band gap increase with increase in Zn doping concentration as given in Table 2. The increase in the optical band gap may be due to the decrease in crystallite size, similar results have been reported earlier [21].
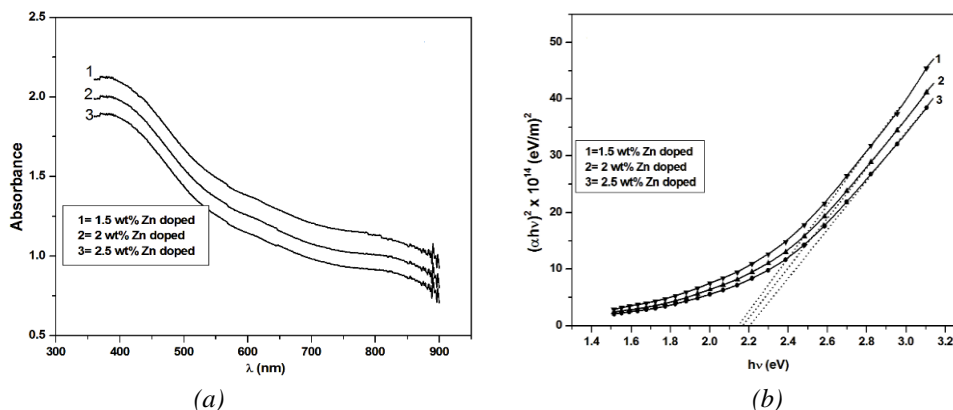

Fig. 4. (a) UV absorption spectra of Zn-doped nanocrystallne PbS thin films prepared at three different concentrations. (b) Plot of $(\alpha h\nu)^2$ vs $h\nu$ of Zn-doped PbS thin films of different doping concentrations.

3.5. Temperature Depedence Electrical Conductivity

The temperature dependence electrical conductivity of Zn doped nanocrystalline PbS thin films of three different doping concentration are shown in Fig. 5. The increase in conductivity with increase in temperature confirms the semiconducting behaviour. The conductivity increases with increase in Zn doping concentration is due to increase free –carrier concentration, which enhances electrical conductivity. The nature of the plots exist two distinct regions: high temperature region and low temperature region. The thermal activation energies of the two regions are calculated using the relation

$$\sigma = \sigma_0 \exp\left(\frac{-E_a}{2kT}\right) \tag{12}$$

where E_a is the activation energy, σ_0 is a constant, k is the Boltzmann's constant and T is the absolute temperature. The calculated activation energies decreases with increase in doping concentration are given in Table 2. Zn doping causes decrease in activation energy of the prepared films, suggesting that there has been band tailing due to increase in doping concentration [28]. The calculated activation energy values of the two regions i.e low and high temperature regions are much smaller than the corresponding band gap values of the Zn doped PbS nanocrystalline thin films. This suggests that these energy levels are thought to be associated with defects levels within the band gap. From thermo e.m.f measurement, the polarity of the thermally generated voltage at the hot end of the films is negative. This shows that the prepared Zn doped PbS nanocrystalline thin films is p-type.

Table 2. Calculated values of optical band gap and electrical conductivity of
Zn doped PbS nanocrystalline thin films at different doping concentrations.

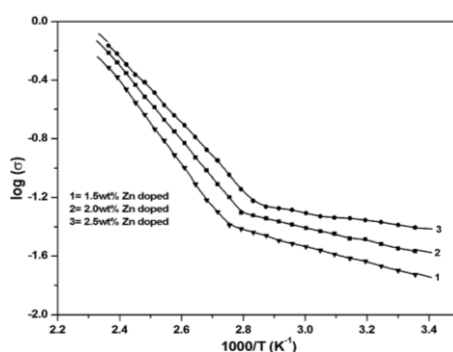| Zn doping concentrations	Thickness of the film (nm)	Optical band gap (eV)	Room temperature conductivity 10^{-4} (Ω^{-1} cm^{-1})	Actication Energy (eV)	
				Low temperature region	High Temperature region
1.5wt%	227	2.15	1.883	0.093	0.046
2.0wt%	223	2.18	2.720	0.079	0.434
2.5wt%	218	2.21	3.935	0.048	0.398

Fig. 5. Plots of variation of log (σ) vs 1000/T of different doping concentration of
nanocrystalline PbS thin films.

3.6. Photoconductive rise and decay studies of nanocrystalline PbS thin film

From Fig. 6, it is observed that for all the Zn doped PbS films at three different concentrations the photocurrent rises very quickly on switching on the light source and then reaches a steady state. Fast rise time response may be attributed to the dominant fast process of photo generation of electron-hole pairs. The current reaches a steady value when the rate of recombination becomes equal to the rate of generation of new carriers and concentration of

carriers reaches a steady value. When the light is switched off, electron-hole pair recombination process dominates, so the photocurrent decays slowly. The photoconductive rise time (τ_r) and decay time (τ_d) are determined from tangents drawn to the photoconductive rise and decay curves. The values are found to decrease with increase in doping concentrations and the estimated values of τ_r and τ_d are tabulated in Table 3. The value of decay constant is determined from the slopes of $\ln I_t$ versus $\ln t$ curves shown in Fig. 7 by using the given relation

$$I_t = I_o(1+at)^{-b} = I_o t^{-b} \tag{13}$$

where I_o is the initial photocurrent at $t=t_{off}$ and I_t is the photocurrent after time t from t_{off} and b is the decay constant.
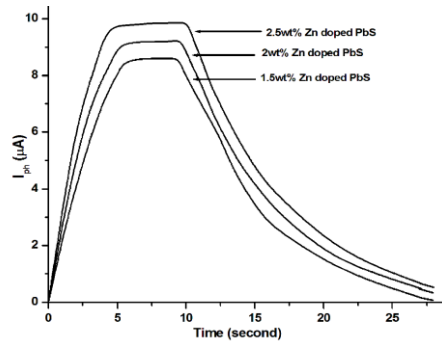

Fig. 6. Rise and decay of photocurrent with time of Zn doped nanocrystallne PbS thin films under illumination of 1700 Lux.
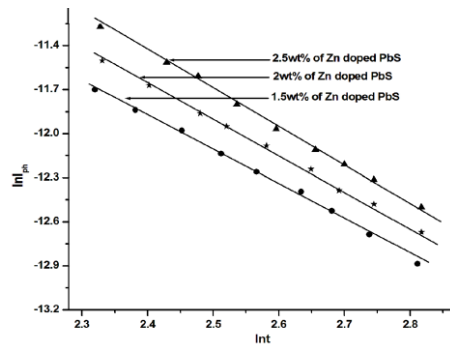

Fig. 7. $\ln I_t$ vs $\ln t$ plots for photoconductive decay of Zn doped nanocrystallne PbS thin films.

Table 3. Various parameters calculated from rise and decay characteristics of Zn doped PbS films under illumination of 1700 Lux.

PbS film	Rise time (τ_r) sec	Decay time (τ_d) sec	Decay constant (b)
1.5wt% Zn doped	4.14	9.42	2.33
2wt% Zn doped	3.59	9.16	2.50
2.5wt% Zn doped	3.18	8.71	2.63

4. Conclusions

In the present investigation, the effect of Zn doped PbS thin film is studied. The XRD studies reveal that the prepared films are polycrystalline in nature with cubic structure. The crystallite size determined from the XRD spectra is found to decrease from 24 nm to 15 nm with increasing doping concentration. From SEM photograph, it is observed that the films are dense, smooth and consist of irregular shapes and sizes. The optical band gap and electrical conductivity increase with increase in doping concentration. The prepared films are found to be p-type as determined by hot probe method.

Acknowledgments

References

[1] A. Hussain, A. Begum, A. Rahman, Indian Journal of Physics **86**(8), 697 (2012).
[2] G. Mandal, T. Ganguly, Indian Journal of Physics **85**, 1229 (2011).
[3] S. Sarmah, A. Kumar, Indian Journal of Physics **84**, 1211 (2010).
[4] S. Devi, M. Srivastava, Indian Journal of Physics **84**, 1561 (2010).
[5] J. Bhadra, D. Sarkar, Indian Journal of Physics **84**, 1321 (2010).
[6] A. Tanaka, S. Onari, T. Arai, Phys. Rev. B **47**, 1237 (1993).
[7] Biljana Pejova, Ivan Grozdanov, Mat. Chem. and Phys. **99**, 39 (2006).
[8] T. Trindade, O. O'Brien, N. L. Pickett, Chem. Mater. **13**, 3843 (2001).
[9] D. Jason Riley, Jonathan P. Waggett, K. G. Upul Wijayantha, J. Mater. Chem. **14**, 704 (2004).
[10] M. Gratzel, Nature **414**, 338 (2001).
[11] D. Cummins, G. Boschloo, M. Ryan, D. Corr, S. N. Rao, D. Fitzmaurice, J. Phys. Chem. B **104**, 11449 (2000).
[12] A. Hussain, A. Begum, A. Rahman, Arab J. Sci. Eng. **38**, 169 (2013).
[13] L. Rajen Singh, S. Bobby Singh, A. Rahman, Chalcogenide letters **10**, 167 (2013).
[14] A. Hussain, A. Begum, A. Rahman, Indian Journal of Physics **86**(8), 697 (2012).
[15] L. Raniero, C. L. Ferreira, L. R. Cruz, A. L. Pinto, R. M. P. Alves, Physica B: Condensed Matter. **405**, 1283 (2010).
[16] M. Sharon, K. S. Ramaiah, M. Kumar, M. Neumann-Spallart, C. Levy, Journal of Electroanalytical Chemistry **436**, 49 (1997).
[17] B. Thangaraju, P. Kaliannan, Semiconductor Science and Technology **15**, 849 (2000).
[18] J. Puiso, S. Tamulevicius, S. Lindross, M. Leskela, V. Snitka, Thin Solid Films **428**, 223 (2003).
[19] Mengting Liu, Wei Li, Yinzhen Wang, Qinyu He, Physica B: Condensed Matter **545**, 245 (2018).
[20] M. G. Faraj, F. A. I. Chaqmaqchee, H. D. Omar, J. Optoelectron. Adv. M. **19**(5), 412 (2017).
[21] Mengting Liu, Qiuquang Zhan, Wei Li, Rui Lei, Qinyu He and Yinzhen Wang, Journal of Alloys and Compounds **792**, 1000 (2019).
[22] K. M. Gadve, S. A. Jodgudri, C. D. Lokhande, Thin Solid Films **245**, 7 (1994).
[23] J. Puiso, S. Tamulevicius, S. Lindross, M. Leskela, V. Snitka, Thin Solid Films **428**, 223 (2003).
[24] R. Yousefi, M. Cheragizade, F. Jamali-sheinic, R. M. Mahmoudian, A. Saaedi, M. N. Huang, Chinese Physics: B **23**, 108101 (2014).
[25] R. Niruban Bharati, S. Sankar, International Journal of Chem Tech. Research **7**, 7 (2014).
[26] B. Baruah, L. Saikia, M. N. Bora, K. C. Sarma, IOSR-JAP **5**(2), 7 (2013).
[27] M. Bedir, M. Oztas, O. F. Bakkaglu, R. Ormanel, Eur. Phys. Jour. B **5**(4) 465 (2005).
[28] J. Tauc, R. Grigorovici, A. Vancu, Phys Status Solidi B **15**, 627 (1966).